

Petrography and geochemistry of middle bhuvan formation Nagaland, India: Implications on depositional environment, provenance, paleoweathering and tectonic settings

Mhabemo Odyuo*, S. Ramasamy, Elizabeth Odyuo, P. Parthasarathy and A. Chinna Durai
Department of Geology, University of Madras, Guindy Campus, Chennai-600025, India
odyuomhabe@gmail.com

Available online at: www.isca.in

Received 12th October 2017, revised 5th January 2018, accepted 20th January 2018

Abstract

Petrography and geochemistry of Middle Bhuvan Formation (Surma group) Nagaland was determined for depositional environment, provenance, paleoweathering and tectonic settings. Six petrographic rock types of quartz rich were identified. Definite micrograding of sediment sequence comprising of fine quartz wacke, siltstone and organic rich clay (upward fining) attest the transportation and deposition of sediments by currents in deeper shelfal environment. Unbent mica flakes with the floating nature of clasts in matrix rich material reveal composition of sediments that reached depositional basin has rich clay matrix and sediments underwent shallow burial diagenesis. The Chemical Index Alteration, Plagioclase Index Alteration and Chemical Index Weathering (CIA, PIA and CIW) indicate moderate weathering in source area. A-CN-K diagram reiterates source rocks had attained moderate weathering. The Al_2O_3/TiO_2 ratio corroborates sediments derivation from felsic rich provenance. The average SiO_2/Al_2O_3 ratio suggests sediments derived from acidic rocks. The discrimination analysis shows sediments falling under the Quartzose sedimentary provenance. The bivariate plot of SiO_2 vs. total $Al_2O_3+K_2O+Na_2O$ indicates sediments deposition under arid to semi-arid paleoclimate. K_2O/Na_2O vs. SiO_2 and SiO_2/Al_2O_3 vs. K_2O/Na_2O diagrams illustrate sediments deposition in active continental margin where sediments are mineralogically, chemically and texturally immature. Thus, quartz rich fine clastics were derived from crystalline source rocks with some contribution from older sedimentaries and deposited in a convergent tectonic setting involving dynamics of Indian subducting plate under Burmese plate in the northeastern India.

Keywords: Depositional environment, provenance, paleo-weathering, tectonic settings, middle Bhuvan formation.

Introduction

The Bengal Basin, its geological evolution that covers Bangladesh and part of eastern India started in the late Mesozoic with the breakup of Gondwanaland and is still continuing¹. The Surma Basin forms a part of the foreland basin of the Himalayan orogen and the Indo-Burma Ranges (active continental margin). Subsidence commenced in pre-Oligocene times continuing until the present as mentioned². The status of the lower Surma Group (Bhuban Formation) of rocks from the standpoint of facies analysis has not yet been firmly established. However, in most published accounts³⁻⁵ the deltaic to shallow marine depositional settings (neritic environment) inferred for the whole of the Surma Group succession has been seen as a paradigm for the stratigraphic, tectonic and sedimentological history of the Bengal Basin. The Pre-Miocene sequence of the Surma Valley constitutes, which are expected to be dominantly marine in nature. On account of the marine influence, this sedimentary sequence is generally attributed to be the facies equivalent of the Memari Formation (Barail Group) of the West Bengal geoprovince. On the other hand the recording of microfossils such as *Bolivina*, *Bulimina*, *Cassigerinella*, *Globigerina* and *Rotalia* from the subsurface sequence found in

Rashidpur and nearby areas of Bangladesh in his paper² is indicative of a more open marine sedimentation.

Study area: The present study was carried out in the Middle Bhubhan formation (450m) (Surma Group, Lower Miocene to Quarternary) located along the road side of National Highway-39 at the entrance gate of Patkai Christian College (Figure-1) (Table-1), having 25°45'12"N Longitude and 93°45'49"E Latitude. The study area falls on the survey of India toposheet No: 83 G/13. Shales interlayered with ribbles, sandstones and siltstones are conspicuous feature of the Group. The present study brings to supportative information in reconstruction of its depositional environment, provenance, paleoweathering and tectonic settings.

Materials and methods

Sampling and analytical procedures: A total of Twenty-eight (28) samples were collected. The samples collected were taken for every 1 meter intervals upto 28 meters i.e. from 0 to 28m height. Thin sections were prepared for representative samples from the road side section where a total of 10 samples were chosen for petrography studies for its composition, texture, and

fabric through slice observation with optical microscopy. An Olympus BX50F4 microscope with Coolpix 990 Nikon automatic camera attachment was used for Petrographic analysis from G.S.I Guindy, Chennai. Major elements of twelve (12) samples were analyzed from NCESS lab Trivandrum Kerala. Trace metal concentrations (Fe, Mn, Cr, Cu, Pb, Zn, Co, Ni and Cd) were estimated using a flame atomic absorption spectrophotometer (Perkin-Elmer AA700) equipped with a deuterium background corrector, available at Department of Applied Geology, University of Madras. Suitable internal chemical standards (Merck Chemicals, Germany) were used to calibrate the instrument.

Results and discussion

Petrography: The Surma Group of Middle Bhubhan (450m) formation, Miocene age exposed in front of the Patkai Christian College entrance gate, Nagaland was examined and found to consist predominantly of poorly indurated fine sandstone, siltstone and clay type showing predominantly angular quartz rich. Micaceous matrix content is considerable. Thus the framework grains of quartz, feldspar and lithic reworked sedimentary fragments are “floating” in the matrix. Lithic fragments are predominantly highly siliceous and finely textured. The original nature of these lithics is dominantly laminated siltstones and mudstones. The identified Petrographic types were examined under Plane polarised light (PPL) indicated by “A” and Cross polarised light (XPL) indicated by “B” as described⁶ scheme of classification of sandstones as shown in Figures 8-13.

Feldspathic quartz wacke (Figure-8, F1): This petrographic type represents the fine sandstone facies of Surma Group and shows a framework of fine grained sub-angular quartz grains with laths of unweathered feldspars, and muscovite mica set in a clay matrix. Feldspar content is considerable and found to be unaltered. Mostly feldspars are alkali orthoclase type showing distinct cleavages. Quartz grains are mostly monocrystalline and found to be assorted. Both very fine quartz and fine quartz are volumetrically equal. Few reworked fine clasts (shales/siltstone) are scattered in the petrographic type. Opaque (mostly magnetite) is seen sporadically. Matrix content is considerable and found to be detritally derived from source rocks. The fine quartz clasts are seen floating in the matrix but very closely with neighbouring grains. The mica flakes are not bent. Perhaps the sediments have settled in a calm depositional environment.

Laminated micaceous siltstone (Figure-9, F3): The framework grains are fine angular quartz grains and micaceous minerals. The micaceous minerals are muscovite mica and chlorite. Even among silt size quartz grains there is distinct variation in grain size (poor sorting). Lamination with clay rich bands is seen. The clay rich bands show rhythmically deposited fine clay alternate with considerable very fine silt size grains. The settlement of micaceous materials shows book like arrangement. No bioturbation is noticed. Grains size is highly

variable between silt and clay rich laminations. It is matrix rich rocks consisting clay, chlorite, and muscovite.

Micaceous laminated siltstone and fine quartz wacke (Figure-10, F9): This Petrographic type is dominantly fine quartz wacke and found alternate with laminations of siltstone and clay. Muscovite mica flakes are good in number and found aligned parallel to the laminations. It also reveals a micro grading as an upward fining sequence starting from quartz rich wacke followed by siltstone and dark argillaceous bands. Quartz grains even within the quartzwacke are highly assorted in grain size and are found to be highly angular. A group of linear fine quartz grains shows faint parallel orientation aligning parallel to flow lines during their settlement in the depositional basin. Though rhythmic deposition is distinctly visible, few micro-cross laminations are sporadically observed here and there. Many opaque heavy minerals are visible, but they are confined to fine quartzwacke laminations. Argillaceous matrix content is volumetrically considerable. The greenish colour matrix may indicate the presence of chlorite clay mineral in the matrix.

Laminated siltstone (Figure-11, F13): Micaceous content is considerable. Some fine clay fragments are scattered in the silt rich layer suggesting feeble current activity in the depositional basin which eroded the already deposited fine clay laminations or they could be reworked from the older sequence. However it looks that they are penecontemporaneous. Few opaque mineral grains are found interspersed in the matrix rich layer. Few quartz grains are coarse and found to be assorted in size. Most of the quartz grains are angular excepting one or two which are sub-rounded. In hand specimen Sample F13 shows distinct laminations of siltstone and dark colour clay. No bioturbated features are noticed in the entire petrographic type thus revealing rhythmic sedimentation.

Lithic argillaceous quartz wacke (Figure-12, F17): This petrographic type is comparatively coarser in grain size. The framework grains are quartz, feldspar and fine grained lithic fragments. The quartz grains are monocrystalline type, highly angular and assorted in texture. Feldspars are mostly microcline exhibiting the typical grid-twinning. There are good number of fine lithic sedimentary fragments (reworked materials from older sequence of Barail and Disang). Most of these lithic fragments are fine siltstone and clay. It is a matrix rich petrographic type and matrix colour is greenish which may reveal the presence of chlorite mineral. Grains of quartz seem to be floating in the argillaceous matrix. However quartz grains are rich in the petrographic type. Few linear delicate plant fragments are noticed along with few garnet grains which are found scattered. Several black opaques materials are found which may be derived mostly from magnetite and ilmenite).

Immature fine grain quartz wacke (Figure-13, F21): This petrographic type is fine grained quartz rich rock exhibiting assorted grain size even among fine quartz grains. The quartz grains are highly angular and monocrystalline. Many reworked

lithic fragments (fine grained siltstone and clay) are seen scattered over the petrographic type. Internally this does not show any laminations revealing this section is made from the fine sandstone layer. It is found to be unfossiliferous. One or two feldspar grains are also observed. This petrographic type is matrix rich which is green in colour (chlorite). Many black grains are found which could be opaques (magnetite and ilmenite). This petrographic variety looks like the clasts have been dumped into the depositional site and the sedimentation rate could be considerably at higher rate.

Geochemistry of sandstones and siltstones (major and trace): The major element compositions of the Surma Group of Middle Bhubhan (450m) formation are quite variable (Table-2). The Surma sandstones of Middle Bhubhan (450m) formation are classified into Fe-sand and Litharenite, subarkose and arkose (Figure-2). The geochemistry of major oxides distribution for Surma Group sediments of Middle Bhubhan (450m) formation shows a decreasing order $\text{SiO}_2 > \text{Al}_2\text{O}_3 > \text{CaO} > \text{Fe}_2\text{O}_3 > \text{MgO} > \text{K}_2\text{O} > \text{Na}_2\text{O} > \text{TiO}_2 > \text{P}_2\text{O}_5 > \text{MnO}$. The trace elements (Table-3), especially the transition elements (Cr and Ni) have higher concentrations range of Cr (94.2–311) ppm, (UCC=35ppm and PAAS=110ppm) and Ni (2.7–170.3ppm), (UCC=20ppm and PAAS=55.0ppm) respectively as compared to the UCC 7 and PAAS 8 values, but have lower concentrations of Co (0.2 -9.8) (UCC=10.0ppm and PAAS=23.0ppm) in the studied sediments. Although felsic source rocks contain comparatively low Cr, Ni, and Co. Some heavy mineral concentrations make uncertainty, e.g. Cr (94.2–311) ppm concentration of sediments are very high possibly due to the high concentrations of chromium spinel, chromite and magnetite or significant ophiolitic component in the paper⁹.

Paleoweathering: The Chemical Index of Alteration ($\text{CIA} = \{ \text{Al}_2\text{O}_3 / (\text{Al}_2\text{O}_3 + \text{CaO}^* + \text{Na}_2\text{O} + \text{K}_2\text{O}) \} \times 100$), was quantified for determination of source rock weathering proposed by¹⁰. Source weathering and elemental redistribution during diagenesis can be assessed using Plagioclase Index of Alteration ($\text{PIA} = \{ (\text{Al}_2\text{O}_3 - \text{K}_2\text{O}) / ((\text{Al}_2\text{O}_3 - \text{K}_2\text{O}) + \text{CaO} + \text{Na}_2\text{O}) \} \times 100$), As proposed by Fedo C.M. et al¹¹ Chemical Index of Weathering ($\text{CIW} = \{ \text{Al}_2\text{O}_3 / (\text{Al}_2\text{O}_3 + \text{CaO} + \text{Na}_2\text{O}) \} \times 100$). The CIA value gives the relative proportions of secondary aluminous clay minerals to primary silicate minerals like feldspars in the mentioned paper^{10,12}. The above equations in the major oxides are expressed in molar proportions and CaO is the content of CaO incorporated in the silicate fraction. The CaO content of the sandstones of the present study varies from 1 to 21.11% with an average of 5.49%. The higher CIA values (76 to 100) in the sedimentary rocks suggests intense chemical weathering in the source region¹³⁻¹⁵ whereas low values (50 or less) indicate the near absence of chemical weathering and also reflect cool and arid conditions¹¹. CIA values of Middle Bhubhan Formation range from 31.73 to 73.25 with an average of 61.39. CIA values range from 50-65 point out weak weathering, whereas 85 to 100 reflects strong weathering. In the present study, the CIA values reveal a moderate weathering in the source area. The molar

proportions of Al_2O_3 , Na_2O and CaO (CaO in silicate fraction) in A-CNK ($\text{A}=\text{Al}_2\text{O}_3$; $\text{CN}=\text{CaO}+\text{Na}_2\text{O}$; $\text{K}=\text{K}_2\text{O}$) ternary diagram evaluates the element mobility during progress of chemical weathering of source material and post depositional chemical modifications of the sandstone and siltstone as published by Nesbitt H. and Young G.M.¹⁰. The A-CN-K diagram plot above plagioclase-potash feldspar joins (Figure-3) which defines a narrow linear trend and the trend line runs slightly at an angle to A-CN edge. This is primarily because removal rates of Na and Ca from plagioclase are generally greater than the removal rates of K from microcline¹⁰ the plots trend towards “A” apex. The plots do not show any inclination towards the K apex, thus indicating that the sandstone and siltstone were not subjected to potash metasomatism during diagenesis. The trend line when extended backward intersects the plagioclase-potash feldspar join near the field of granite (potential source rock). Linear weathering trend suggests steady state of weathering conditions where material removal matches with production of weathering material proposed by Nesbitt R.W.¹⁶.

Provenance: The geochemical signatures of clastic sediments have been used to find out the provenance Characteristics as proposed by many researchers^{8,17-20}. $\text{Al}_2\text{O}_3/\text{TiO}_2$ ratio of most sediment is essentially used to infer the source rock compositions because the $\text{Al}_2\text{O}_3/\text{TiO}_2$ ratio increases from 3 to 8 for mafic igneous rocks, from 8 to 21 for intermediate rocks, and from 21 to 70 for felsic igneous rocks²¹. In Surma group of Middle Bhubhan Formation, $\text{Al}_2\text{O}_3/\text{TiO}_2$ ratios range from 20.69 to 28.09. The $\text{Al}_2\text{O}_3/\text{TiO}_2$ ratio of this study suggests that the source rocks are probably from felsic rocks. $\text{SiO}_2/\text{Al}_2\text{O}_3$ ratio is sensitive to recycling and weathering processes and mainly used for understanding the sediment maturity²². The average $\text{SiO}_2/\text{Al}_2\text{O}_3$ ratio in unaltered igneous rocks range from ~ 3.0 (basic) to ~ 5.0 (acidic), while values of >5.0-6.0 in sediments are an indication of progressive maturity²³. The result points to immature nature of the sediments. The average $\text{SiO}_2/\text{Al}_2\text{O}_3$ ratio is 5.29 suggesting that the sediments are derived from acidic rocks. The discriminant function diagram proposed by Roser B.P. and Korsch R.J.²² and Roser B.P. and Korsch R.J.²³ permits separation of provenance into four major groups: (P1) mafic igneous (P2) intermediate igneous (P3) felsic igneous and (P4) quartzose sedimentary. The oxides of Ti, Al, Fe, Mg, Ca, Na and K are effectively used to differentiate the sediments into four provenance zones. The discrimination diagram of Surma rocks of Middle Bhubhan Formation suggests that the sediments are probably derived from intermediate igneous and Quartzose sedimentary provenance (Figure-4).

Paleoclimate: Major elements data provide useful information regarding the climatic conditions that prevailed during the deposition of sediments and sedimentary rocks²⁴. The bivariate plot of SiO_2 against total $\text{Al}_2\text{O}_3+\text{K}_2\text{O}+\text{Na}_2\text{O}$ for palaeoclimatic inference during deposition of the sediments in the basin is well recognized by many workers. Suttner L.J. and Dutta P.K.²⁴ proposed a binary SiO_2 wt. % versus $(\text{Al}_2\text{O}_3+\text{K}_2\text{O}+\text{Na}_2\text{O})$ wt. %

diagram to constrain the climatic condition during sedimentation of siliciclastic sedimentary rocks. On this diagram, the sediments plot essentially in the field of semi-humid to semi-arid climate (Figure-5) indicating that the sediments of the study area are deposited under arid to semi-arid paleoclimate. In addition, palaeoclimate and chemical maturity of sediment material delivered to the basin can also be deduced from chemical composition of the sediments. The Al_2O_3/TiO_2 ratio (<20 in humid conditions and >30 in arid climatic conditions) can be used as a climate indication for the source area. The average Al_2O_3/TiO_2 ratio of 23.93 implies a semi-arid condition for the provenance area.

Tectonic setting: The major element-based on discrimination diagrams for various tectonic setting are widely used^{22,25}. In the bivariate, including discriminant functions, are based on immobile and variably mobile major elements, including Na_2O and K_2O . The tectonic setting discrimination diagrams can

provide reliable results for siliciclastic rocks that have not been strongly affected by post-depositional weathering/metasomatism/metamorphism. In view of the uncertainties of the major element-based discrimination diagrams, the present work have considered almost all the available major element-based discrimination diagrams to arrive at the best possible inference on tectonic setting of the provenance of the sandstones and siltstone of the present study. In the widely used K_2O/Na_2O versus SiO_2 wt. % diagram proposed by Roser B.P. and Korsch R.J.²² the sandstones and siltstone clearly plot in active continental margin field (Figure-6), but in the modified version of the same bivariate diagram proposed by Murphy S.²⁶. In the SiO_2/Al_2O_3 versus K_2O/Na_2O diagram proposed by Maynard J.B. and Valloni R.²⁷ of the sandstones and siltstone plot in active continental margin field (Figure-7). In active continental margin settings, sediments are deposited at subduction arc basins, strike-slip margins, and in proximal portions in back-arc basins²⁸.

Table-1: Generalised Stratigraphic Succession of Nagaland, Eastern Himalaya after^{29, 30}.

Age	Group/Sub Group	Formation and thickness in MTS.	Lithology
Pleistocene to Holocene	Alluvium	Alluvium	Gravels, silts, and clays.
Pleistocene	Dihing	Dihing (300-1600m)	Pebbles, cobbles and boulders of Sandstone in ferruginous coarse sandy matrix.
Pliocene to Pleistocene	Dupitila	Namsang (800m)	Sandstone, coarse occasionally pebbly and gritty with mottled clay bands.
Miocene to Pliocene	Tipam	Girujan Clay (1300-2300m)	Mottled clays, shales of varied colours with medium to fine grained sandstone.
		Tipam s.st	Massive sandstone, medium to coarse grained with current bedded structures.
Miocene	Surma	Bokabil (400m)	Alternation of shales with silt- stone and sandstone.
		Upper Bhubhan (400m)	Alternation of sandstone and shale.
		Middle Bhubhan (450m)	Silty shale with sand lenticles, sandstone medium grained soft with current ripples.
Late Eocene to Oligocene	Barail	Renji (900m)	Sandstone medium to thick bedded, fined grained, well sorted, occasional carbonaceous shales.
		Jenam (850m)	Shale with subordinate sandstone, sandstone occur as lenticular bodies and as thin bands
Cretaceous to Eocene	Disang	Upper (1800-3000m)	Dark grey, splintery shale with noncalcareous siltstone and silty sandstone
		Lower	Epimetamorphosed sediments of slates, phyllite with lenticular limestone beds. Ophiolites.

Table-2: Major Oxide's variation (in wt %) of Surma Group sediments.

Sample	F1	F2	F4	F8	F11	F13	F15	F18	F21	F24	F27	F28
SiO ₂	76.11	68.65	73.73	69.3	67.19	71.05	56.39	76.59	66.84	72.1	71.82	42.09
TiO ₂	0.49	0.6	0.52	0.59	0.66	0.64	0.51	0.55	0.41	0.56	0.58	0.47
Al ₂ O ₃	11.8	14.18	12.64	14.24	15.11	13.37	11.25	11.38	11.25	12.99	13.32	12.18
MnO	0.02	0.03	0.02	0.03	0.03	0.03	0.62	0.03	0.2	0.02	0.03	0.64
Fe ₂ O ₃	3.45	4.72	3.85	4.9	5.01	4.31	3.11	3.86	2.96	4.13	4.53	6.36
CaO	1	1.75	1.58	1.65	1.6	1.68	21.11	1.09	11.28	1.53	1.47	20.12
MgO	1.24	3.3	2.6	3.21	3.38	3	2.26	2.04	2.23	3.1	2.95	9.86
Na ₂ O	1.48	1.24	1.35	1.33	1.17	1.3	1.33	1.58	1.24	1.49	1.35	0.75
K ₂ O	1.83	2.59	2.24	2.63	2.82	2.49	1.77	1.79	2.07	2.46	2.51	2.87
P ₂ O ₅	0.11	0.12	0.11	0.13	0.12	0.14	0.14	0.1	0.1	0.12	0.14	2.37
LOI	2.48	2.7	1.3	1.98	2.82	1.96	1.49	0.98	1.3	1.45	1.25	2.22
Total	100.01	99.88	99.94	99.99	99.91	99.97	99.98	99.99	99.88	99.95	99.95	99.93
CIA	73.25	71.76	70.97	71.74	73	70.97	31.73	71.84	43.54	70.33	71.42	33.91
PIA	60.87	65.67	70.89	72.22	68.09	72.01	32.24	73.79	41.43	66.48	56	34.37
CIW	80.08	79.49	78.02	79.58	81.61	78.5	29.7	78.22	42.3	77.71	79.31	30.85
SiO ₂ /Al ₂ O ₃	6.45	4.84	5.83	4.87	4.45	5.31	5.01	6.73	5.94	5.55	5.39	3.46
Al ₂ O ₃ /TiO ₂	28.1	23.63	24.31	24.14	22.89	20.89	22.06	20.69	27.44	23.2	22.97	25.91
Al ₂ O ₃ /SiO ₂	0.16	0.21	0.17	0.21	0.22	0.19	0.2	0.15	0.17	0.18	0.19	0.29
Fe ₂ O ₃ +MgO	4.68	8.02	6.45	8.11	8.39	7.31	5.37	5.9	5.19	7.23	7.48	16.22
K ₂ O+Al ₂ O ₃	13.63	16.77	14.88	16.87	17.93	15.86	13.02	13.17	13.32	15.45	15.83	15.05
K ₂ O/Na ₂ O	1.24	2.09	1.66	1.98	2.41	1.92	1.33	1.13	1.67	1.65	1.86	3.83
K ₂ O/Al ₂ O ₃	0.16	0.18	0.18	0.18	0.19	0.19	0.16	0.16	0.18	0.19	0.19	0.24

Table-3: Trace element concentration of Middle Bhuban formation Surma group in ppm.

Sample No.	Depth in meters	Fe	Mn	Ni	Co	Cu	Cr	Pb	Zn
F1	0	18508	312	2.7	0.7	58.4	311	60	190.9
F2	1	20580	361	101.5	0.5	57.8	223.8	74	285.9
F3	2	13600	279	103.7	9.1	50.9	167.7	25.7	248.4
F4	3	18760	247	102.4	5.6	44.9	183.1	59.7	232.6
F5	4	18475	391	108.9	5.3	35.6	206.1	96.1	296.5
F6	5	22097	459	47.4	7.8	43	210.6	43.8	276.9
F7	6	19343	267	42.5	9.8	52.9	234.8	1.1	224.4
F8	7	19097	317	53	5.4	49.3	128.8	79.2	192.6
F9	8	19356	311	14.3	5.8	41.3	137.5	26.9	26.9
F10	9	17316	264	104.4	7.4	19.1	131.8	21	149.3
F11	10	18708	267	158.9	3.7	14.1	127.4	46	284.3
F12	11	18844	276	114.3	6.1	27.7	147.1	29.3	183.2
F13	12	17634	320	105	4.9	14.5	153.5	20.5	167.1
F14	13	16509	308	134.3	2.3	22.1	163.1	27.2	174.5
F15	14	15725	208	130.9	2.7	12.5	184.9	21.1	169.2
F16	15	17419	250	118.4	7.8	6.7	193.6	25	150.2
F17	16	15069	278	158.6	9.7	73	183.7	24.1	160.7
F18	17	17389	298	135.8	7.8	50.2	16.6	16.6	216.1
F19	18	19260	233	170.3	4.9	50.6	141.6	40.4	162.1
F20	19	19294	303	168.7	9.4	57.5	166.8	25.2	159.8
F21	20	16806	494	132.9	4.8	49.2	161.4	25.6	159.6
F22	21	16806	735	154	4.5	39.6	99.9	23.9	151.5
F23	22	17930	212	131.5	3.5	30.1	124.1	11.9	162.8
F24	23	14929	201	101.2	0.2	16.7	114.3	17.5	141.1
F25	24	15800	236	101.2	2.3	31	99.6	11.2	131.6
F26	25	16064	225	79.5	2	27.9	136.8	20.5	139.6
F27	26	15372	175	105.7	4.6	47.4	94.2	21.3	154.6
F28	27	17366	328	128.1	3.8	96.5	113.7	33.4	240.5
	MAX.	22097	735	170.3	9.8	96.5	311	96.1	296.5
	MIN.	13600	175	2.7	0.2	6.7	94.2	1.1	131.6
	AVG.	17658.4	315.5	106.1	5.08	40.79	162.34	34.18	131.6

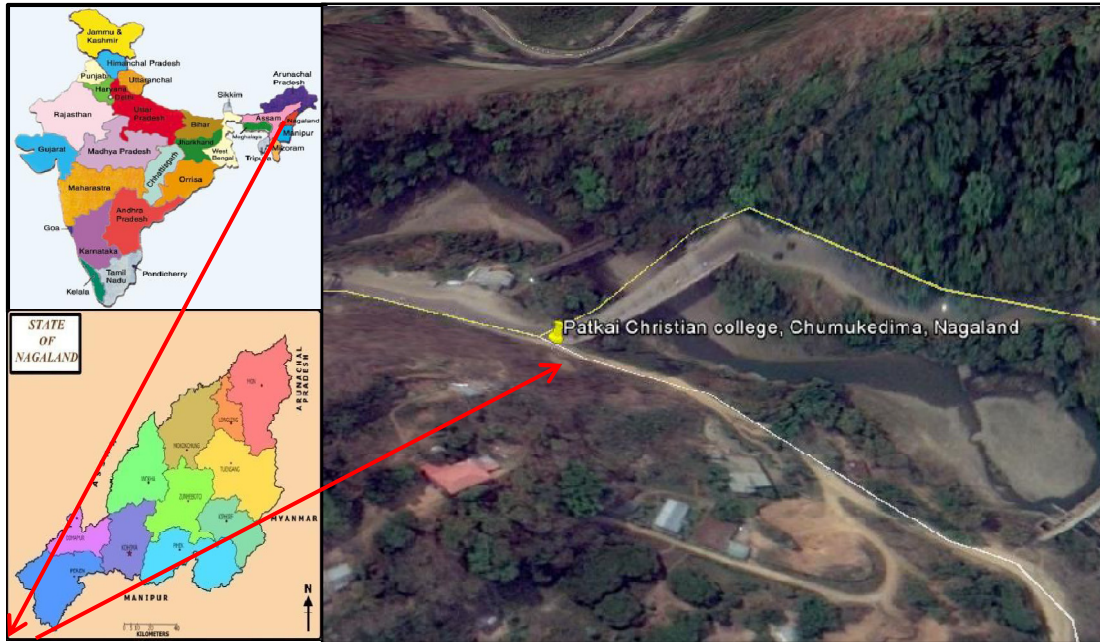


Figure-1: Location Map of the study area Middle Bhuban formation (Surma group).

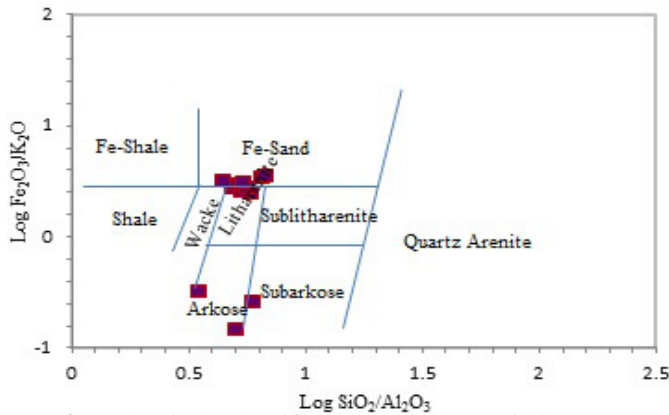


Figure-2: Chemical classification of the Middle Bhuban formation, (Surma group).

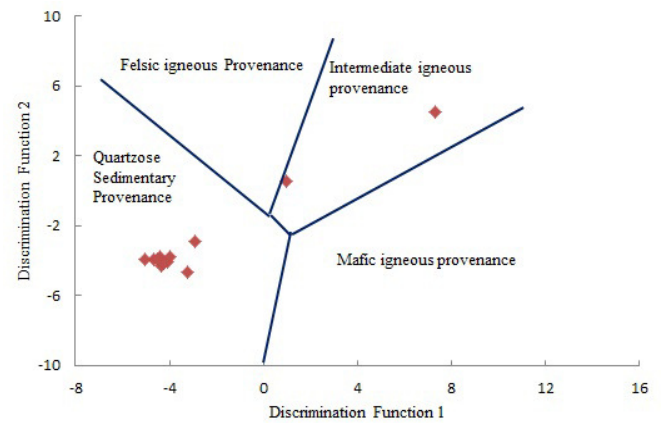


Figure-4: Provenance discrimination diagram for Middle Bhuban formation, (Surma group).

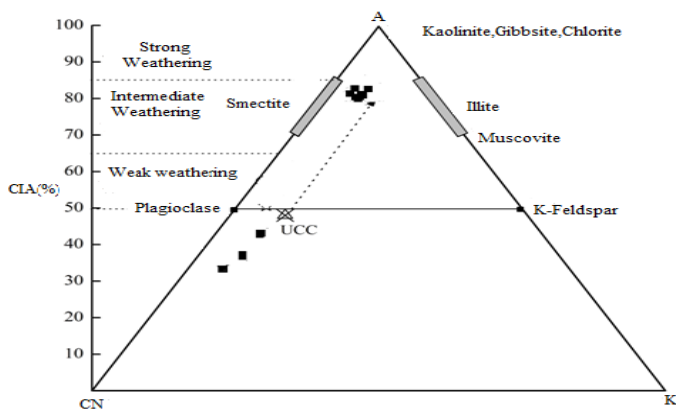


Figure-3: A-CN-K ternary diagram [A = Al₂O₃; CN = (CaO+Na₂O); K = K₂O] CIA=Chemical Index of Alteration, showing weathering trends in the Middle Bhuban formation (Surma group).

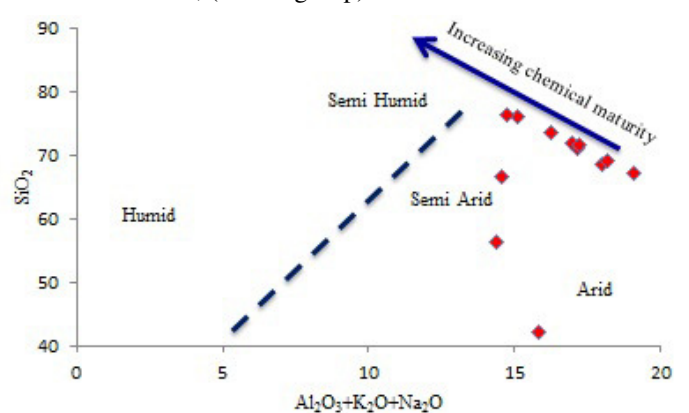


Figure-5: Chemical maturity of Middle Bhuban formation, (Surma group), their palaeoenvironment of deposition based on SiO₂ wt.% versus (Al₂O₃+K₂O+Na₂O) wt.% bivariate diagram.

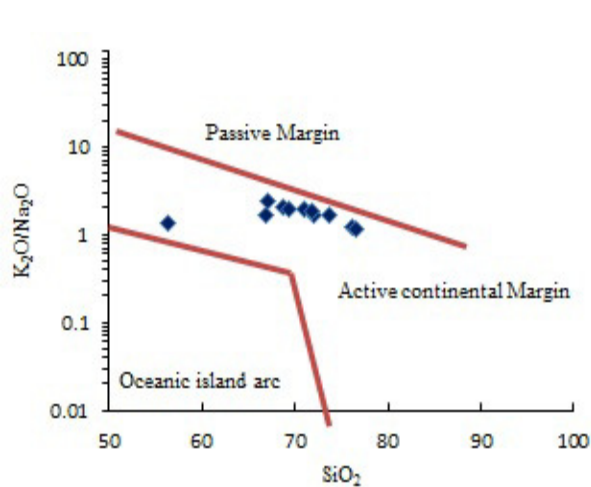


Figure-6: Tectonic setting discrimination diagrams K_2O/Na_2O vs SiO_2 .

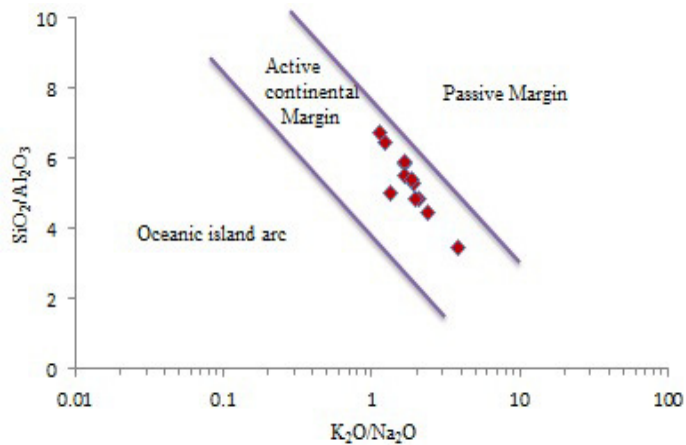


Figure-7: Tectonic setting discrimination diagrams K_2O/Na_2O vs. SiO_2/Al_2O_3 plots.

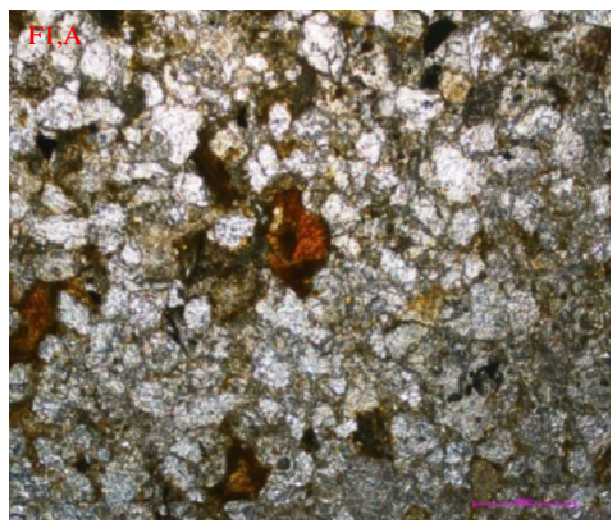


Figure-8: Felspathic quartz wacke.

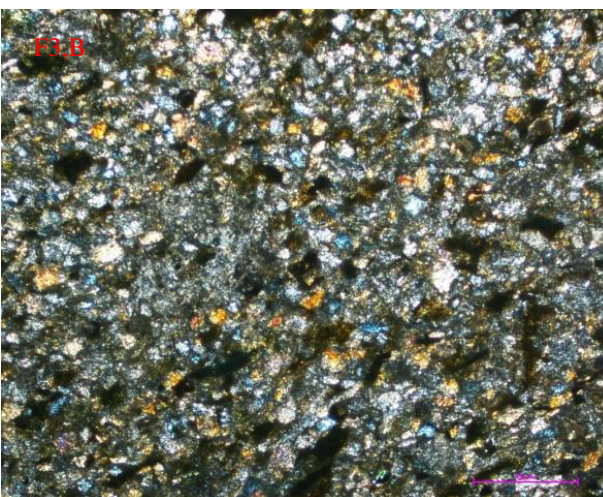
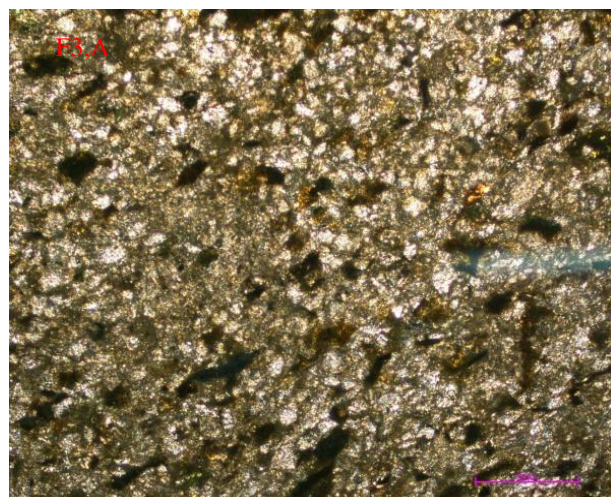


Figure-9: Laminated micaceous siltstone.

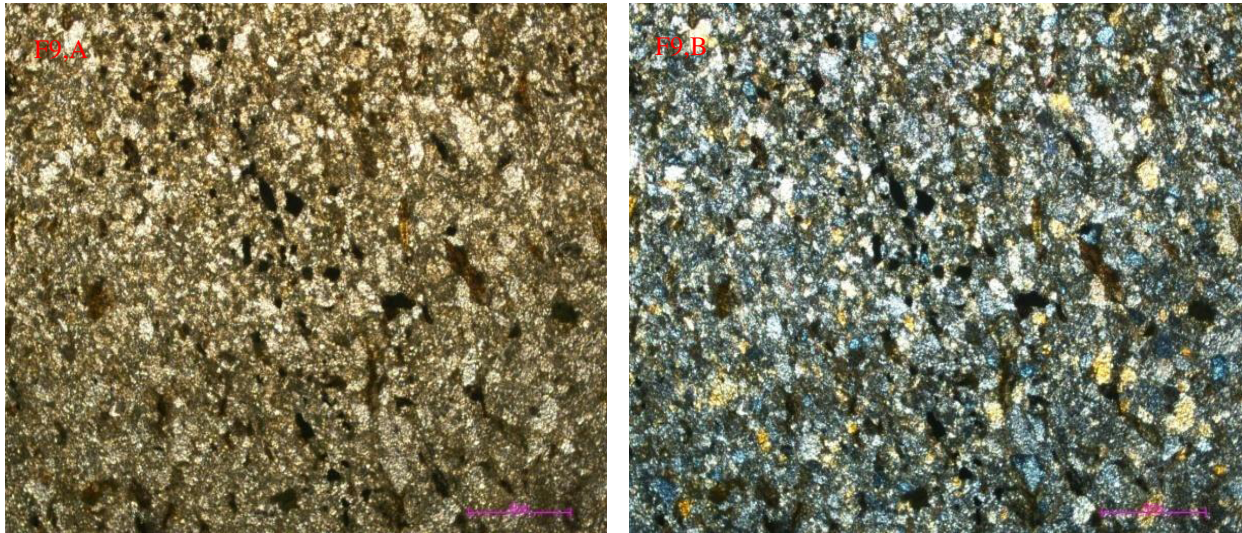


Figure-10: Micaceous laminated siltstone and fine quartz wacke.

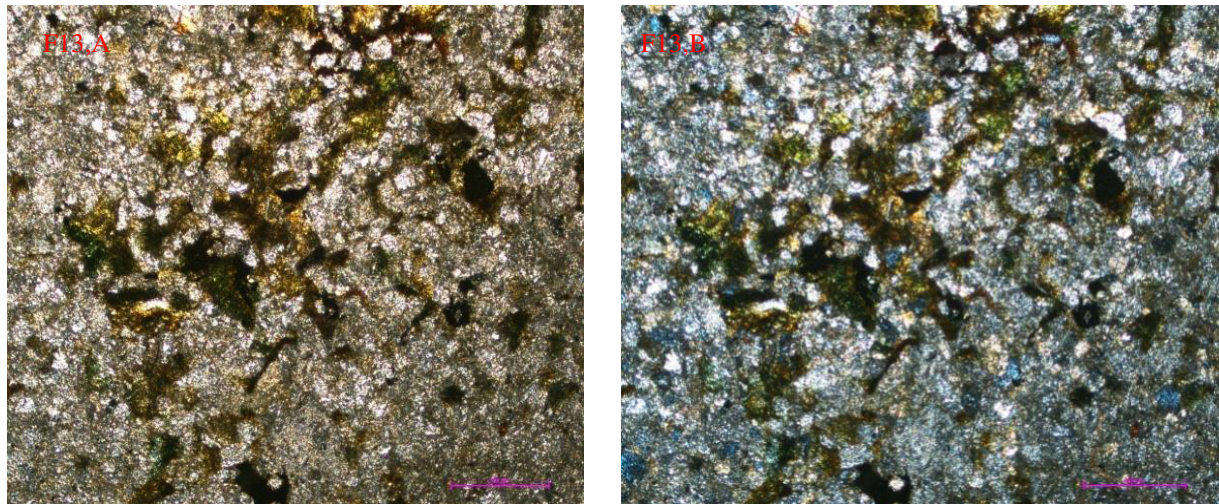


Figure-11: Laminated siltstone.

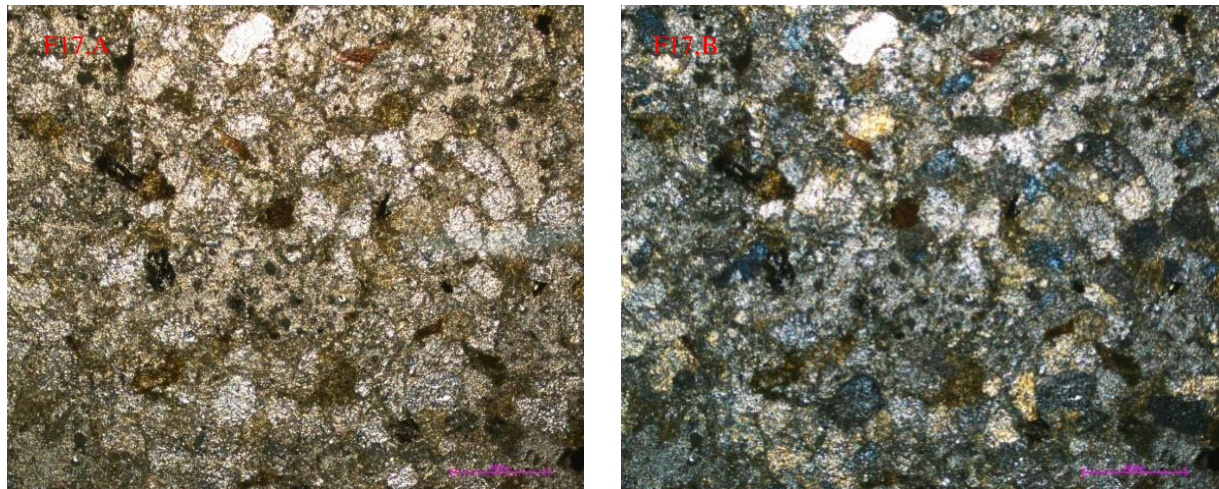


Figure-12: Lithic argillaceous quartz wacke.

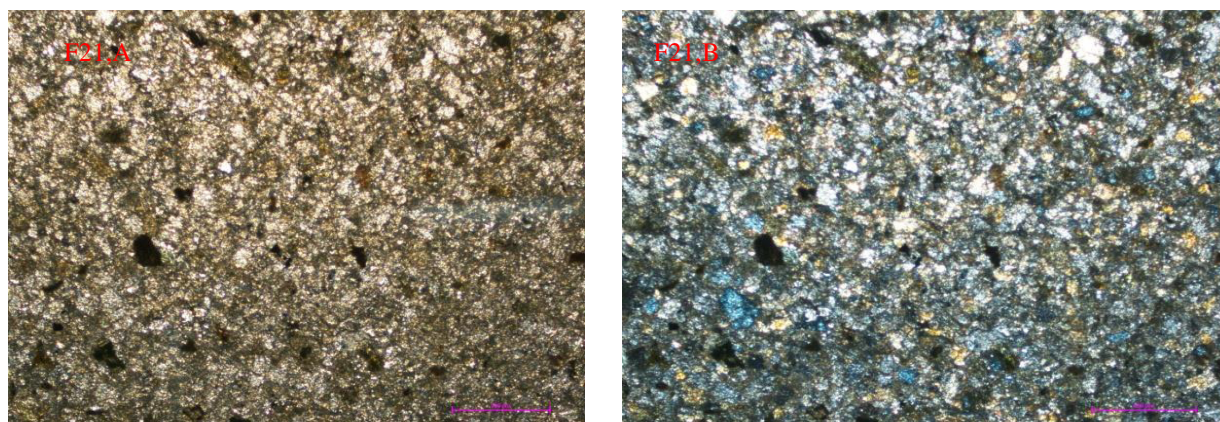


Figure-13: Immature fine grain quartz wacke.

Conclusion

From the study area of the Surma group of Middle Bhubhan (450m) formation, a general graded bedding feature among these fine clastics could be visualized: fine grained sandstone, siltstone and top clay unit. They are rhythmically deposited. The sequences are not bioturbated in general excepting at one or two instances at top level units. Hence in all likelihood the depositional environment could be a deep marine setting and sediments were moved by turbidity currents and the lithofacies are interbedded sandstone and shales/siltstones. Ripple marks could be found on deep sea floor when currents move over the seafloor. Hence these features are not reliable evidences for assigning deep or shallow water. The sedimentary rate was comparatively much higher as sediments are rarely bioturbated.

Petrographic study reveals the dominance of quartz grains. The quartz grains are surrounded in shape in Feldspathic Quartz Wacke and very angular in siltstones. Micaceous material is considerable and mostly represented by muscovite mica and chlorite. The laminations are rhythmically deposited and alternate between clays and siltstones. Rarely laminations are displayed with fine Quartz Wacke, Micaceous Siltstone and clays- a fining upward sequence. This reveals that the depositional conditions rather very similar to deep marine environments, perhaps the sediments were moved by turbidity currents that operated in the deep sea. In general the grains are loosely packed or exhibiting a floating features in the matrix rich Petrographic types. Further the mica flakes in the fine grained petrographic types are found to be unbent and straight. Hence it is likely that the sediments have undergone a shallow burial diagenesis. Based on floating nature of the fine sand grains in the matrix rich sandstone, besides the absence of bent micas in the micaceous rich sandstones and siltstones, it is inferred that these Surma Group of Middle Bhubhan (450m) formation sediments have undergone shallow burial diagenesis.

Geochemically the Surma Group sediments of sandstone and siltstone of Middle Bhubhan (450m) formation are classified as lithic wacke, Fe -sand, and subarkose wacke. CIA values and A-CN-K diagram suggests that the clastics rocks of the present

study have undergone moderate weathering of felsic rocks. The tectonic setting ratios are consistent with active continental marginal settings, suggesting an unstable continental setting. Such a setting should produce mineralogically, chemically and texturally immature sediments. Thus the active continental margin setting at the convergence of the Indian and Burma plates has generated and deposited the sediments. The Geochemical analytical results suggest that the sediments are mineralogically, chemically and texturally immature. Thus, the overall geochemical investigation proves that the sediments were sourced from active continental margin setting due to subduction of the Indian Plate under the Burmese plate in the North-eastern India and is concluded that the fine grain sediments such as siltstone and sandstone have settled in a deep marine environment.

Acknowledgement

The authors wish to thank the authority of Madras University, Department of Geology, Chennai, India, for allowing us in carrying out on the research topic, and acknowledge the help rendered to us for the analysis work done in CESS Kerala, India.

References

1. Alam M. (1989). Geology and depositional history of Cenozoic sediments of the Bengal Basin of Bangladesh. *Palaeogeography, Palaeoclimatology, Palaeoecology*, 69, 125-139.
2. Holtrop J.F. and Keizer J. (1970). Some aspects of the stratigraphy and correlation of the Surma Basin wells, East Pakistan. *ECAFE Mineral Resources Development Series*, 36, 143-154.
3. Ganguly S. (1983). Geology and Hydrocarbon Prospects of Tripura-Cachar- Mizoram Region. *Petroleum Asia Journal*, 6(4), 105-109.
4. Johnson S.Y. and Alam A.M.N. (1991). Sedimentation and tectonics of the Sylhet trough, Bangladesh. *Geological Society of America Bulletin*, 103(11), 1513-1527.

5. Shamsuddin A.H.M. and Abdullah S.K.M. (1997). Geologic evolution of the Bengal Basin and its implication in hydrocarbon exploration in Bangladesh. *Indian Journal of Geology*, 69, 93-121.
6. Dott R.H. (1964). Wacke, greywacke and matrix-what approach to immature sandstone classification?. *Jour. Sed. Petrol.*, 34(3), 625-632.
7. Condie K.C. (1993). Chemical composition and evolution of the upper continental crust: Contrasting results from surface samples and shales. *Chemical Geology*, 104, 1-37.
8. Taylor S.R. and McLennan S.M. (1985). *The Continental Crust: Its Composition and Evolution*. Blackwell Scientific Publications, Oxford, 312.
9. Nagarajan R., Roy P.D., Jonathan M.P., Lozano R., Kessler F.L. and Prasanna M.V. (2014). Geochemistry of Neogene sedimentary rocks from Borneo Basin, East Malaysia: Paleo-weathering, provenance and tectonic setting. *Chemie der Erde-Geochemistry*, 74(1), 139-146.
10. Nesbitt H. and Young G.M. (1982). Early Proterozoic climates and plate motions inferred from major element chemistry of lutites. *Nature*, 299, 715-717.
11. Fedo C.M., Nesbitt H.W. and Young G.M. (1995). Unraveling the effects of potassium metasomatism in sedimentary rocks and paleosols, with implications for paleoweathering conditions and provenance. *Geology*, 23(10), 921-924.
12. Young R.J., Carleson P.D., Hunt T. and Walker J.F. (1998). High yield and high throughput TEM sample preparation using focused ion beams. In *Proceedings of the 24th ISTFA Conference*, Materials Park, Ohio, USA: ASM, 329, 332.
13. Fadipe O.A., Carey P.F., Akinlua A. and Adekola S.A. (2011). Provenance, diagenesis and reservoir quality of the Lower Cretaceous sandstone of the Orange Basin, South Africa. *South African Journal of Geology*, 114(3-4), 433-448.
14. Srivastava V., Gusain D. and Sharma Y.C. (2013). Synthesis, Characterization and Application of Zinc Oxide Nanoparticles (n-ZnO). *Ceram. Int.*, 39(8), 9803-9808.
15. Újvári G., Varga A., Raucsik B. and Kovács J. (2014). The Paks loess-paleosol sequence: A record of chemical weathering and provenance for the last 800ka in the mid-Carpathian Basin. *Quaternary International*, 319, 22-37. doi.org/10.1016/j.quaint.2012.04.004
16. Nesbitt R.W., Hirata T., Butler I.B. and Milton J.A. (1997). UV laser ablation ICP-MS: Some applications in the earth sciences. *Geostandards and Geoanalytical Research*, 21(2), 231-243.
17. Condie K.C., Phillip D.N.J. and Conway C.M. (1992). Geochemical and detrital mode evidence for two sources of Early Proterozoic sedimentary rocks from Tonto Basin Supergroup, central Arizona. *Sedimentary Geology*, 77(1-2), 51-76.
18. Cullers R.L. (1995). The controls on the major-and trace-element evolution of shales, siltstones and sandstones of Ordovician to Tertiary age in the Wet Mountains region, Colorado, USA. *Chemical Geology*, 123(1-4), 107-131.
19. Madhavaraju J. and Ramasamy S. (2002). Petrography and major element geochemistry of Late Maastrichtian-Early Palaeocene sediments of Tiruchirapalli, Tamil Nadu- Palaeoweathering and Provenance Implications. *Geological Society of India*, 59(2), 133-142.
20. Armstrong-Altrin J.S., Lee Y.I., Verma S.P. and Ramasamy S. (2004). Geochemistry of sandstones from the upper Miocene Kudankulam Formation, southern India: Implications for provenance, weathering, and tectonic setting. *Journal of sedimentary Research*, 74(2), 285-297.
21. Hayashi K.I., Fujisawa H., Holland H.D. and Ohmoto H. (1997). Geochemistry of ~ 1.9 Ga sedimentary rocks from northeastern Labrador, Canada. *Geochimica et Cosmochimica Acta*, 61(19), 4115-4137.
22. Roser B.P. and Korsch R.J. (1988). Provenance signatures of sandstone-mudstone suites determined using discriminant function analysis of major-element data. *Chemical geology*, 67(1-2), 119-139.
23. Roser B.P. and Korsch R.J. (1986). Determination of Tectonic Setting of Sandstone-Mudstone Suites using SiO₂ content and K₂O/Na₂O ratio. *Journal of Geology*, 94(5), 635-650.
24. Suttner L.J. and Dutta P.K. (1986). Alluvial sandstone composition and paleoclimate, I. Framework mineralogy. *Journal of Sedimentary Research*, 56(3).
25. Bhatia M.R. (1983). Plate tectonics and geochemical composition of sandstones. *The Journal of Geology*, 91(6), 611-627.
26. Murphy S. (2000). Production of nitric oxide by glial cells: regulation and potential roles in the CNS. *Glia*, 29(1), 1-13.
27. Maynard J.B. and Valloni R. (1982). Ho Shing Ju, Composition of Modern Deep Sea Sands from Arc Related Basin. *J. Geol. Soc. Am. Spec. Publ*, 10, 551-561.
28. Alvarez N.C. and Roser B.P. (2007). Geochemistry of black shales from the Lower Cretaceous Paja Formation, Eastern Cordillera, Colombia: Source weathering, provenance, and tectonic setting. *Journal of South American Earth Sciences*, 23(4), 271-289.
29. Evans P. (1932). Tertiary succession in Assam. *Trans. Min. Geol. Inst. India*, 27(3), 155-260.
30. Rao R.A. (1983). Geology and hydrocarbon potential of a part of Assam-Arakan basin and its adjacent region. *Petroliferous Basins of India. Petroleum Asia Jour*, 6, 127-158.